ELSEVIER

A New Generation of High Performance Concrete: Concrete with Autogenous Curing

Silvia Weber and Hans W. Reinhardt
Stuttgart University and FMPA BW, Stuttgart, Germany

The literature and site data on the efficiency of curing are controversial regarding its effect on the mechanical properties of high strength concrete. The traditional methods of curing may fail in cases of concrete with a low water/binder ratio and with addition of silica fume. Hydration proceeds quickly, the hydrated cement paste is very dense, and water from the outside cannot reach the interior of the concrete to achieve complete hydration. Replacing 25% by volume of the aggregates by prewetted lightweight aggregates creates water storage inside the concrete, which supports continuous wet curing. The purpose of this article is to introduce a new type of high performance concrete. The materials used and their properties are shown, and the mixing procedure is given. The most important mechanical properties of the concrete under various curing conditions and the microstructure of the hardened cement paste were investigated. The results show that the method of introducing a water reservoir can be successfully applied to obtain high performance concrete with improved properties while being relatively insensitive to curing. Advanced Cement Based Materials 1997, 6, 59–68. © *1997 Elsevier Science Ltd.*

KEY WORDS: Compressive strength, Curing, Degree of hydration, High performance concrete, High strength concrete, Lightweight aggregates, Microstructure, Portland cement, Shrinkage

High strength concrete can be made using a high cement content and a low water/cement ratio, and by the addition of highly reactive pozzolans such as silica fume. The result is a compact structure of the hardened cement paste (HCP) and the interface between the paste and the aggregate. There are some conflicting aspects with regard to curing of high strength concrete. During the hydration of the concrete a shortage of water occurs, such that an insufficient amount of water from the exterior reaches the interior of a concrete member to ensure complete hydration [1]. The unfavorable effect of water shortage, combined with the heat of hydration and self-desiccation, affect the mechanical properties and durability. Decreased compressive strength [2], higher porosity [3], porous zones around the aggregates [3], and sensitivity to cracks [4] were observed. Wet curing or storage in fog for 6 days does not noticeably improve the properties of high strength concrete [5].

A new approach has been used, which introduces a certain amount of lightweight expanded clay aggregates (LWA) with a high moisture content. These porous LWA particles are uniformly distributed throughout the matrix and act as an internal water reservoir. As soon as the hydration process leads to shortage of water in the cement paste there is a humidity gradient. Water from the LWA is transported first by capillary suction [6] and later by vapor diffusion and subsequent capillary condensation from the LWA to the cement paste, thereby supporting continuous hydration. New hydration products fill the pores or microcracks, which might have occurred had self-desiccation proceeded. The result of using such a pre-soaked lightweight aggregate is a concrete that is not sensitive to deficient curing. The structure of the hardened cement paste is more compact and fewer microcracks are observed.

Material Properties and Mixtures

The cement is a rapid hardening Portland cement of type CEM I 42.5 [7]. Silica fume was added as a slurry having a specific gravity of about 1.4 kg/L; 50% of the mass was water. A sulphonated naphthalene-formaldehyde condensate was used as a superplasticizer. Two types of aggregates were used: rounded sand and gravel from the upper Rhine valley with a maximum size of 16 mm, and LWA with grain size of 4–8 mm. The LWA has a dry density of 1420 kg/m^3 and a porosity of about 50%. The moisture content after 24 hours of submersion is 20.2% by mass. The amount of LWA introduced represents 25% of the total volume of aggregates, replacing completely the 4- to 8-mm fraction.

Address correspondence to: Hans-Wolf Reinhardt, Institut fur Werkstoffe im Bauwesen, Universitat Stuttgart, Pfaffenwaldring 4, D70550 Stuttgart, Germany.
Received July 23, 1996; Accepted April 28, 1997

ISSN 1065-7355/97/$17.00
PII S1065-7355(97)00009-6

Advn Cem Bas Mat
1997;6:59–68

TABLE 1. Mixture proportions

Component	Amount	Unit
CEM I 42.5 R	450	kg/m^3
Water[a]	150	L/m^3
Silica fume[b]	45	kg/m^3
Superplasticizer	13.6	L/m^3
Retarder	1.75	L/m^3
Aggregates	**Amount**	**Unit**
Fraction 0/2	471	kg/m^3
Fraction 2/4	260	kg/m^3
Fraction 4/8 LWA	234	kg/m^3
Fraction 8/16	567	kg/m^3
W/B	0.30	

Note: [a]Total water including the water of the silica fume slurry and admixtures; [b]dry mass.

TABLE 2. Curing conditions

Code	Curing Condition
NK = DIN 1048 [9]	6 days submersed in water, then in air 20°C ± 1°C, 65% RH
KR	In air 20°C ± 1°C, 65% RH
KK	In air, temperature varying between 15°C and 25°C, RH varying between 40% and 45%
KL	Sealed in aluminum and polyamid foils

The water/binder ratio of the mix is 0.30. When adding the water to the mix the water content of the slurry W_{Slurry}, the superplasticizer $W_{Superplasticizer}$, and the retarder $W_{Retarder}$, and adherance of the LWA on the surface $W_{surface}$ were considered so that the water added to the mixture W_{added} was equal to:

$$W_{added} = W_{total} - W_{Superplasticizer} - W_{Retarder} - W_{Slurry} - W_{surface}. \quad (1)$$

Table 1 shows the mixture composition. The mixing procedure is as follows. After dry mixing of the normal density aggregates for 1 minute, half the amount of W_{added} is added. After mixing for another minute the LWA is added, followed by the slurry and then the cement. While continuing the mixing, the rest of the W_{added}, retarder, and superplasticizer are added, in 2-minute intervals, followed by a 3-minute final mixing.

The density of the fresh concrete is 2250 kg/m^3. Therefore, in spite of containing LWA, the concrete cannot be classified according to the German Standard DIN 1045 [8] as a lightweight concrete and has to be considered a normal weight concrete. The workability was measured according to the German Standard DIN 1045 using a flow table. Minutes after mixing it had a value of $a_{10} > 500$ mm. The concrete shows a uniform distribution of LWA in cement paste (Figure 1). Floating of LWA during mixing or agglomeration of LWA in the hardened concrete was not observed.

One hundred millimeter cubes were cast and stored in a fog room at 20°C for 24 hours. The specimens then

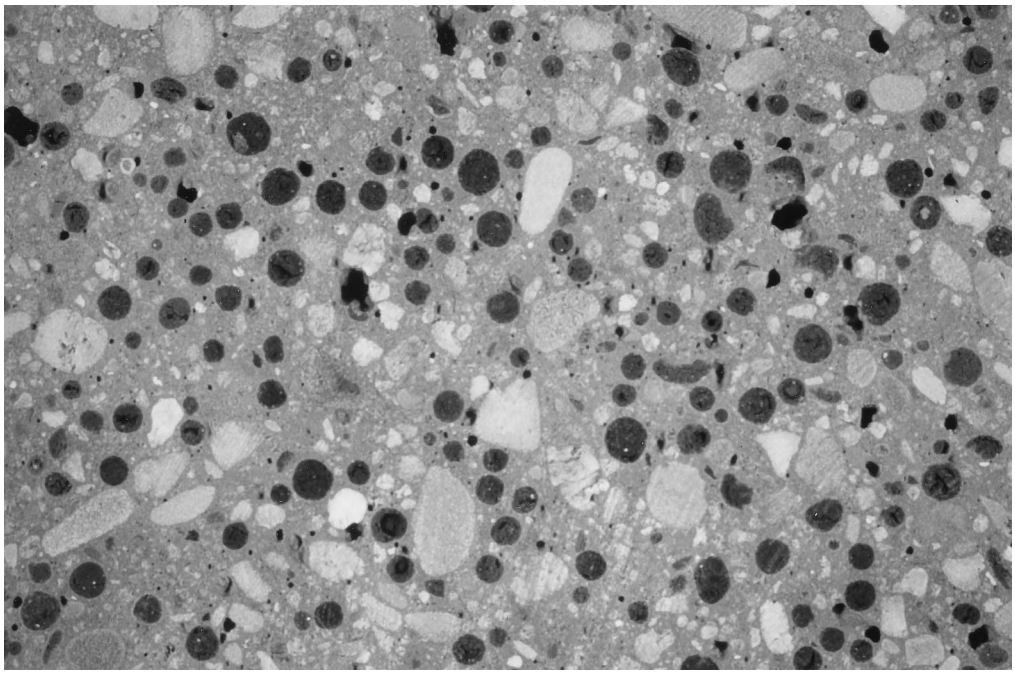

FIGURE 1. High strength concrete with a blend of aggregates.

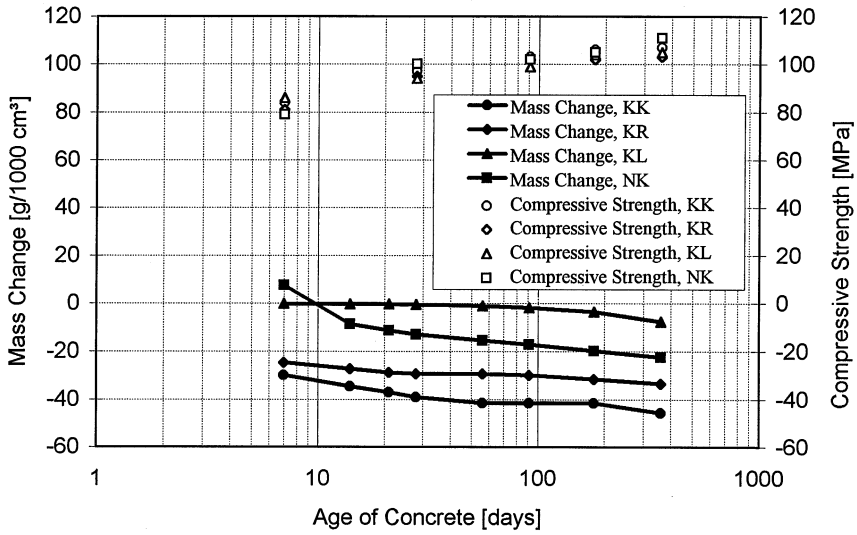

FIGURE 2. Mass change and compressive strength.

were demolded. The cubes were stored under different curing conditions as shown in Table 2. Cubes cured according to the German Standard DIN 1048 [9] achieved a mean compressive strength $f_{c,100,28}$ = 104.0 MPa after 28 days.

Young's modulus is about 34 GPa and was determined on cylinders having a diameter of 150 mm and height of 300 mm cured according to the German Standard DIN 1048 [9].

Tests Performed

Mechanical Properties

The mass of the 100-mm cubes stored under the different curing conditions was regularly monitored up to 360 days, and the compressive strength was determined at 7, 28, 91, 180, and 360 days.

Microscopic Aspects

Samples were taken from the interior of the 100-mm cubes stored under curing condition KK (see Table 2). Some of the samples were dried in an oven at 105°C until they reached a constant mass. Another series of samples was stored above phosphor-pentoxide in a desiccator at 20°C until the physically bound water was extracted.

For the determination of the porosity of samples dried at 105°C the apparent dry density ρ_{dry} was measured. Then the samples were mechanically milled and the density ρ was determined using a helium pycnometer. Considering the porosity of the LWA grains p_{LWA}, the volume fraction of the LWA v_{LWA}, the porosity of the normal density aggregates p_{ag}, and the volume fraction of the normal density aggregates v_{ag}, the porosity of the concrete p_c without the intrinsic porosity of the aggregates becomes:

$$p_c = (1 - \rho_{dry}/\rho) \cdot 100 - p_{LWA} \cdot v_{LWA} - p_{ag} \cdot v_{ag}. \quad (2)$$

In addition, the porosity and pore size distribution of particles of samples stored in a desiccator were measured with the aid of mercury intrusion. To eliminate the influence of LWA porosity, the samples were crushed into small pieces, and particles containing only cement paste and sand grains were selected manually. The specific gravity of the mercury was 13.5, and the contact angle was 141.3°. To obtain a better understanding of the porous structure, the results of the mercury intrusion are given as a differential distribution of the pore volume versus pore radius. Logarithmic scales are used. By plotting $dV/d \log r$ versus $\log r$ the area below the distribution curves corresponds to pore volumina.

Differential thermal analyses are commonly performed on binder paste. For the X-ray diffraction analysis mortar with small plastic spheres replacing the aggregates is used. To show the influence of the moisture stored in the LWA it was necessary to perform the investigations directly on the concrete. Crushing the samples into fine particles and sieving them through a

TABLE 3. Densities of concrete and porosity of concrete without intrinsic porosity of aggregates

Age of Concrete (days)	Apparent Unit Mass (kg/m³)	Density (kg/m³)	Porosity (%)
28	2120	2680	13.0
56	2150	2710	12.9
91	2110	2660	10.5
180	2150	2630	10.5
360	2180	2670	10.3

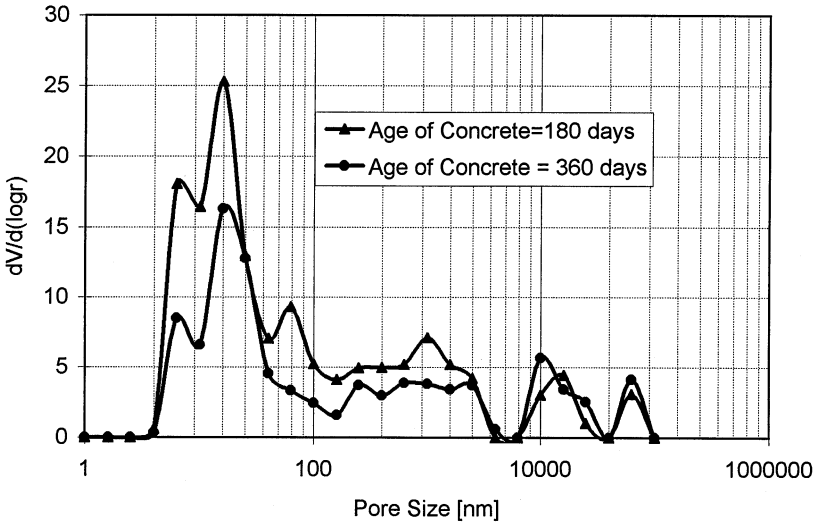

FIGURE 3. Pore size distribution.

mesh size <0.063 mm eliminated all normal density and lightweight aggregates. Thus, samples enriched with hydrated cement paste were obtained. These were subjected to the thermal and X-ray diffraction analyses.

The degree of hydration was calculated taking into account the amount of chemically bound water. The amount of chemically bound water was calculated from the results of the simultaneous thermal analyses of differential thermal analysis (DTA) and thermal gravimetry (TG) and related to the determined cement content of the samples. The cement content of the samples was calculated from investigations on the cement used, slurry, normal density and light-

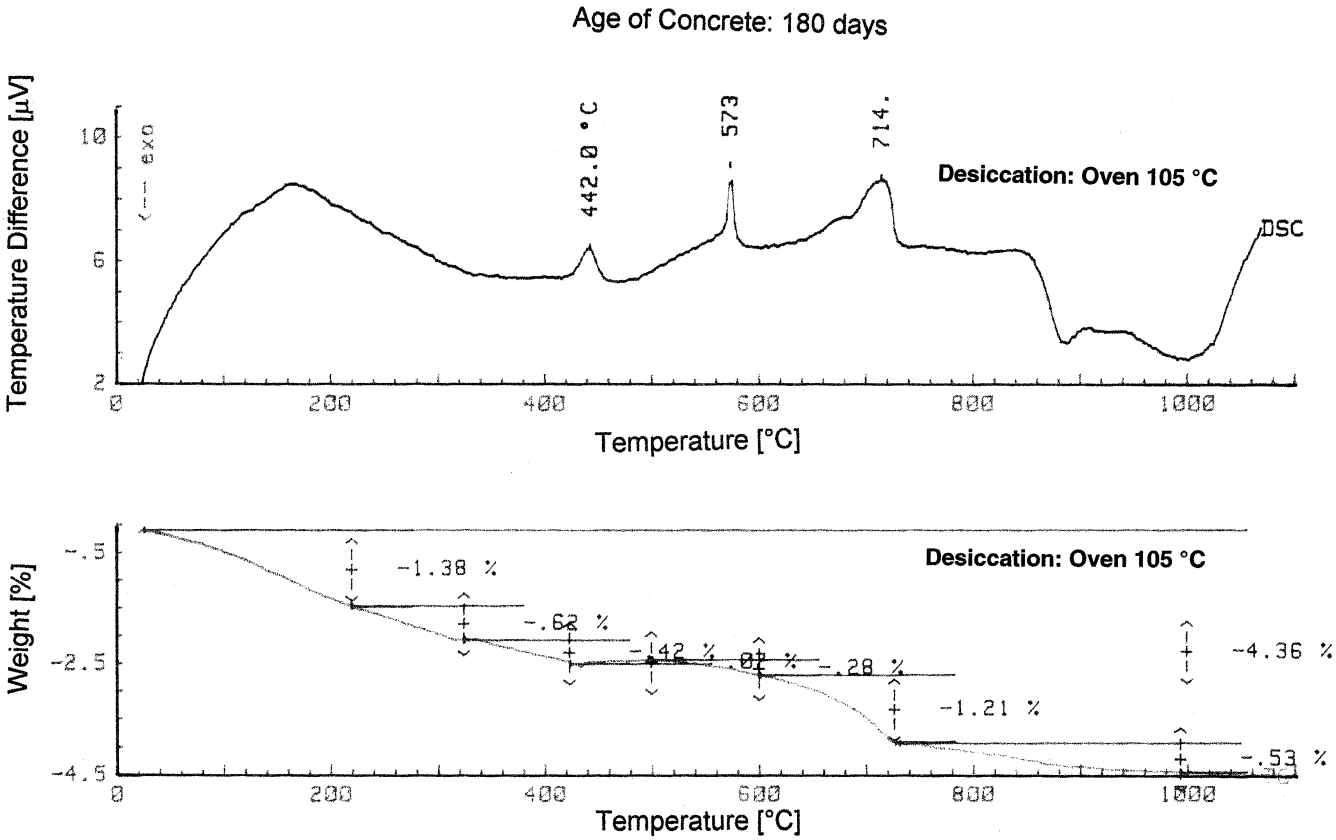

FIGURE 4. DTA and TG results of desiccation: oven 105°C, age of concrete 180 days.

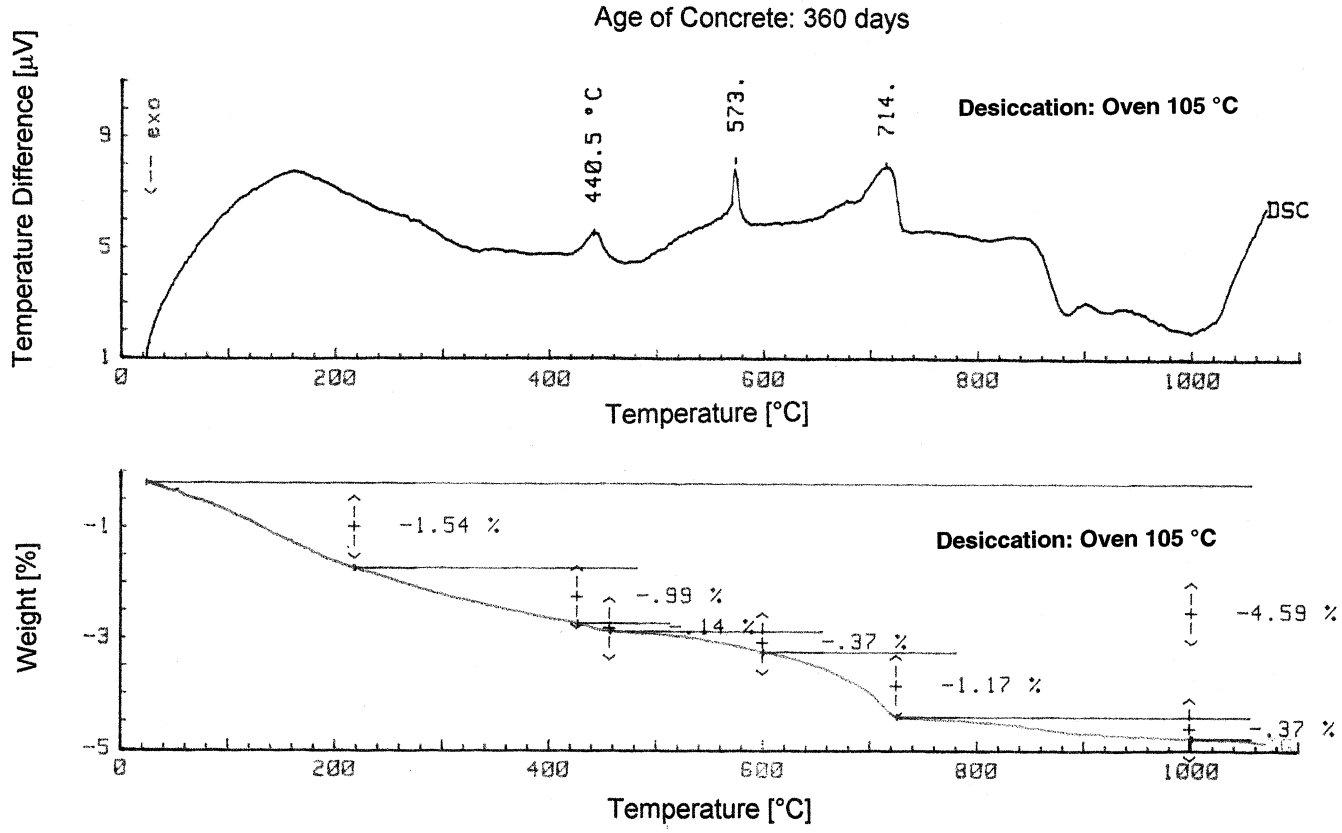

FIGURE 5. DTA and TG results of desiccation: oven 105°C, age of concrete 360 days.

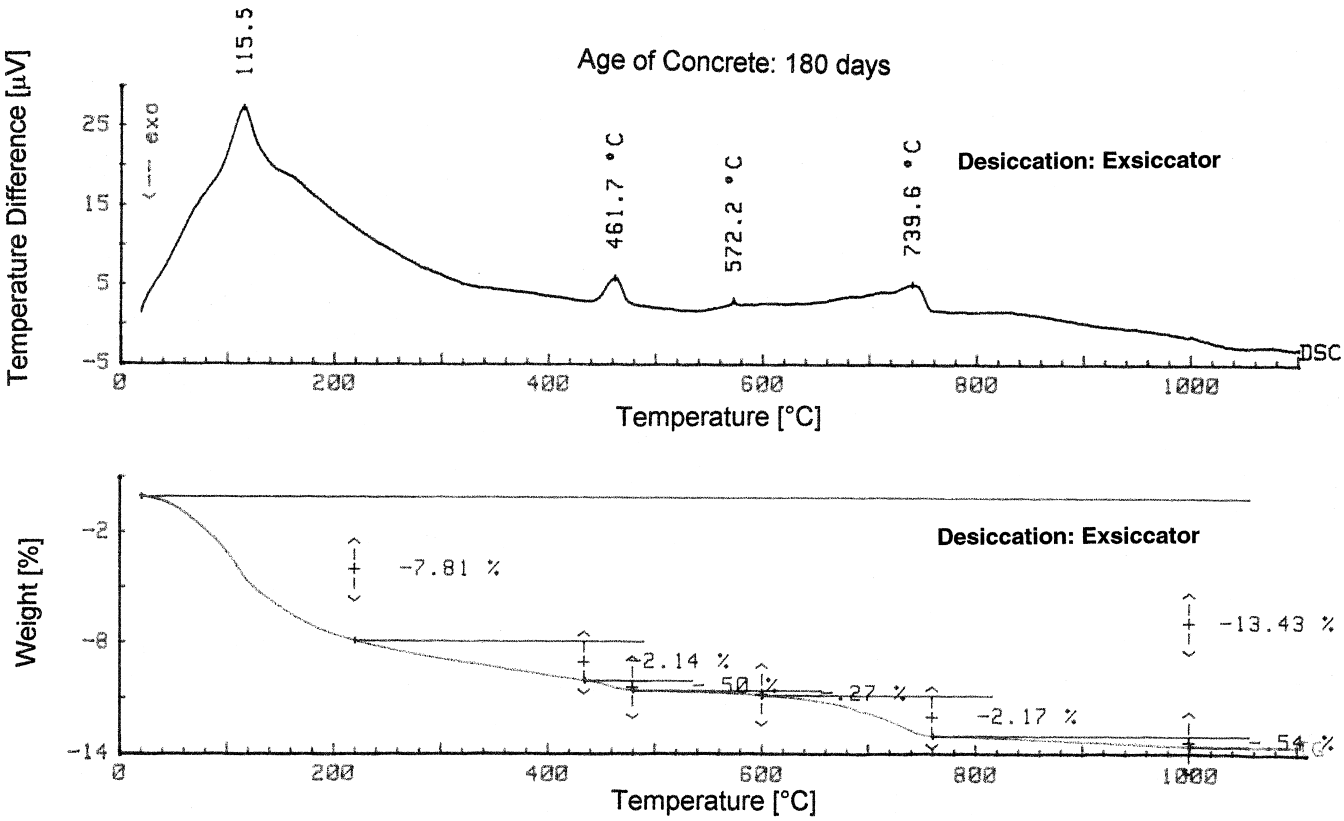

FIGURE 6. DTA and TG results of desiccation: Exsiccator, age of concrete 180 days.

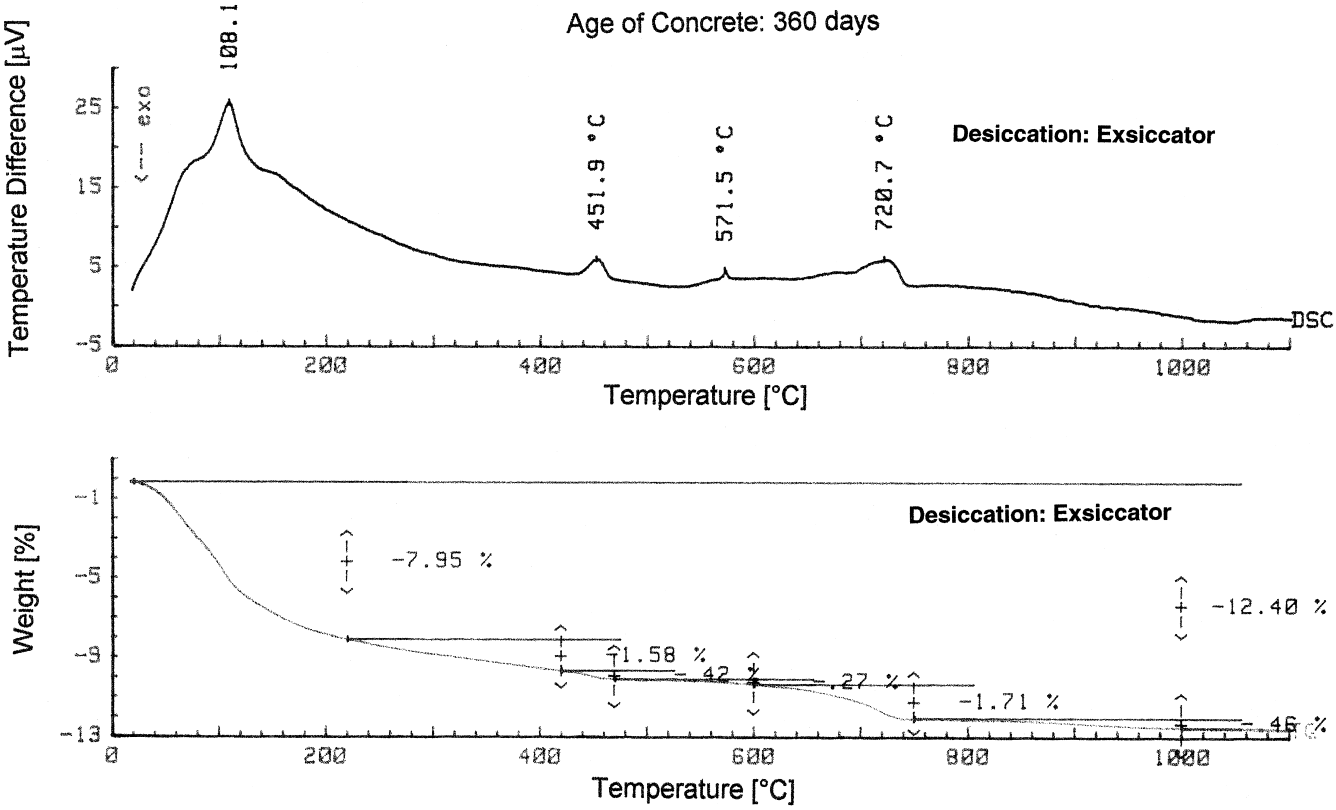

FIGURE 7. DTA and TG results of desiccation: Exsiccator, age of concrete 360 days.

weight aggregates, and amounts of unsoluble parts of SO_3 and CaO. The investigations were carried out on the materials as delivered and without loss of ignition [10].

X-ray diffraction shows the chemical composition of C-S-H, ettringite, and calcium hydroxide. The results can be separated into two widths of reflecting angles. The angles from 9° to 23° show mainly hydration products such as ettringite, portlandite, vesuvianite, and C-S-H phases of the afwillite type. To show clearly the different peaks, the ordinate was chosen to be 1000. The angles from 23° to 35° show mainly C_3S, C_2S, and types of C-S-H phases different than those noted previously. The peaks are related to the cement content of the samples determined by DTA.

Petrographic analysis using fluorescence microscopy was carried out on a thin section taken from the interior of a 48-day-old, 100-mm cube stored in KR (see Table 2) for 28 days and then insulated in aluminum and plastic foils. The thin section was made from a 50 × 50 × 15 mm block cut from the interior of the cube. The section was polished on the surface and vacuum impregnated with an epoxy containing a yellow fluorescent dye. The thin section covered an area of about 50 × 30 mm, and its thickness was 20 to 25 µm.

Results

The mass change and compressive strength of the 100-mm cubes under different curing conditions are shown in Figure 2. Table 3 shows the porosity of the concrete at different ages and Figure 3 the pore size distribution at 180 and 360 days. Figures 4 through 7 show the results of DTA and TG for the cement paste at different ages of concrete for the two types of drying. Calculation of the degree of hydration is given in Table 4. The chemical composition of the concrete is shown in Figures 8 and 9. Figure 10 shows the fluorescence microscopic result of petrographic analysis.

Discussion

Mass Change

The cubes immersed in water for 6 days absorbed a small amount of water during that time, which was lost during the first days of exposure to a relative humidity (RH) of 65% (see Fig. 2). At 14 days a mass loss was observed. This leads to the presumption that, during a limited period of wet curing, the amount of stored water is located mostly at the surface layer and, hence,

TABLE 4. Results of TG and DTA for single samples

Mode of Desiccation		Exsiccator		Oven 105°C	
Age of Concrete (days)		**180**	**360**	**180**	**360**
As delivered	Loss of ignition	13.43	12.41	4.36	4.59
	Unsoluble	34.92	45.01	67.23	68.63
	Amount of SO_3	1.26	1.03	0.67	0.75
	Amount of CaO	27.02	21.39	13.71	14.17
Without loss of ignition	Unsoluble	40.34	51.38	70.29	71.93
	Amount of SO_3	1.46	1.18	0.7	0.79
	Amount of CaO	31.21	24.42	14.34	14.85
Cement content	Unsoluble	55.31	43.08	22.13	20.31
calculated from:	SO_3 without loss of ignition	55.75	43.46	22.42	20.63
	Average value	55.53	43.27	22.27	20.47
Aggregate content	Average value	44.47	56.73	77.73	79.53
Results from TG	20-220°C	7.81	7.95	1.38	1.54
	220-600°C[a]	2.41	1.85	1.32	1.36
	420-490°C[b]	0.50	0.42	0.15	0.14
	From CO_2	2.17	1.71	1.21	1.17
Water content of	20-220°C	0.19	0.19	0.19	0.19
cement + aggregates	220-600°C[a]	0.34	0.32	0.29	0.29
before hydration	420-490°C[b]	0.106	0.082	0.04	0.04
Water content of	20-220°C	7.62	7.76	1.19	1.35
cement + aggregates	220-600°C[a]	2.07	1.53	1.03	1.07
after hydration	420-490°C[b]	0.39	0.34	0.11	0.10
Content of chemically	20-220°C	13.72	17.93	5.34	6.59
bound water related	220-600°C[a]	3.73	3.53	4.62	5.23
to 100 g cement	420-490°C[b]	0.71	0.78	0.48	0.49
	Content of portlandite	2.92	3.21	1.99	2.03
	Total amount of chemically bound water	18.16	22.25	10.44	12.32
	Content of chemically bound water[a]	17.45	21.47	9.96	11.83
	Content of calcium carbonate	4.90	4.90	7.21	7.81
Calculation of the	Water in concrete at t = 0	150.00	150.00	150.00	150.00
degree of hydration (α)	Water chemically bound for $\alpha = 1$	121.50	121.50	121.50	121.50
	Water chemically bound measured	82.00	100.00	47.00	55.00
	Degree of hydration	0.67	0.82	0.39	0.46

Note: [a]Not taking into account the amount coming from portlandite; [b]taking into account the amount coming from portlandite.

it cannot reach the interior of the cube. After 360 days, the mass loss is approximately 22 g per cube.

Exposing the cubes to air from the beginning showed that the mass loss is higher the lower the RH of the environment is. The mass loss is relatively high during the first 7 days. At 360 days for curing conditions of 45% and 65% RH, the mass loss was 45.7 and 33.6 g, respectively.

For sealed cubes the lowest mass loss was measured.

Compressive Strength

The average value of the compressive strength at 28 days reached 98.0 MPa for sealed cubes, 99.0 MPa for curing at 65% RH, and 101.0 MPa for curing at 45% RH (see Fig. 2). Thus, at this age of concrete none of the series reached the standard compressive strength.

Regardless of the curing, a continuous increase in compressive strength with increasing age of concrete can be observed. At 360 days the sealed cubes achieved the lowest value of 109.0 MPa and the cubes stored at 45% RH reached 112.0 MPa. For wet curing the compressive strength at 360 days was 115.0 MPa.

Porosity

Porosity measurements (Table 3) indicate a decrease of total porosity with later age of concrete, underlining the more compact structure of the cement paste.

Supplementary information about the structure of the paste is given by the distribution of pore size (Fig. 3). For samples cured in KK (see Table 2), the relative volume of pores is smaller at 360 days than at 180 days. The number

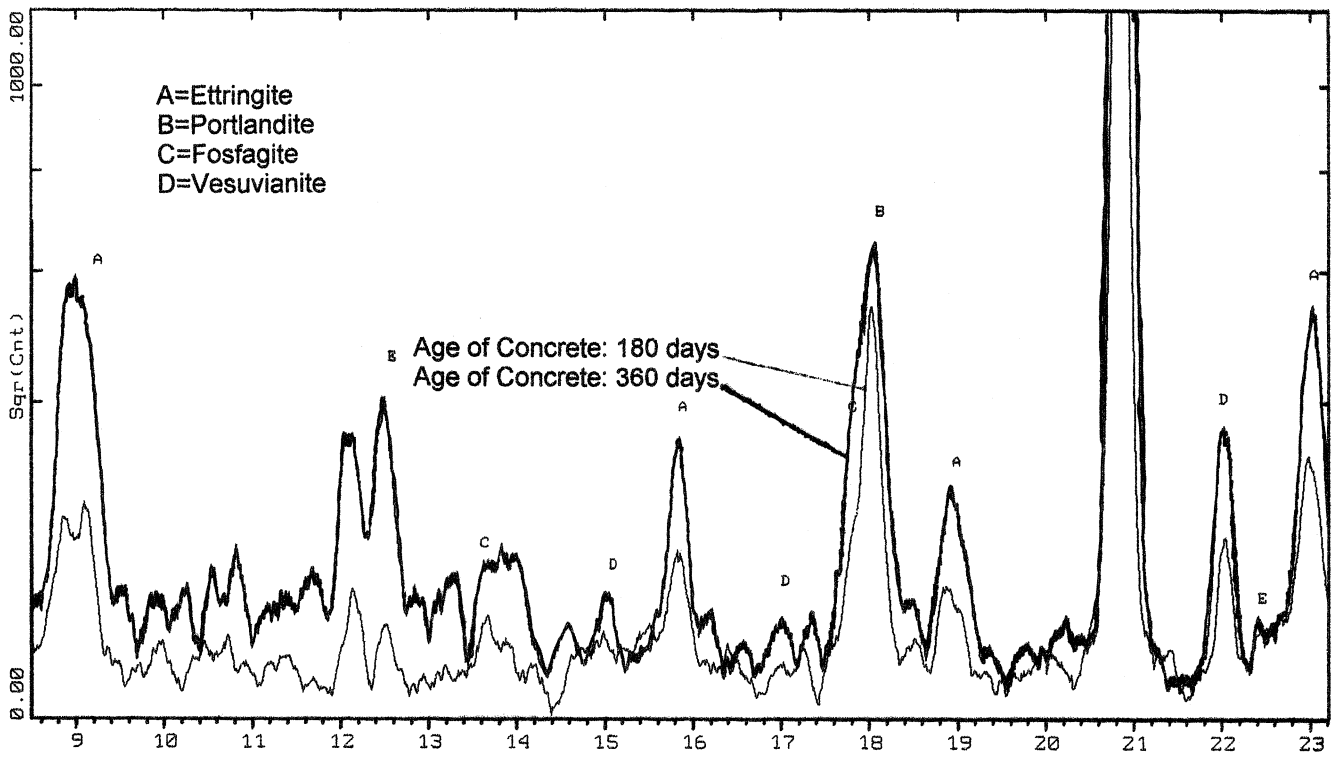

FIGURE 8. X-ray diffraction reflecting angles from 9° to 23°, age of concrete 180 and 360 days.

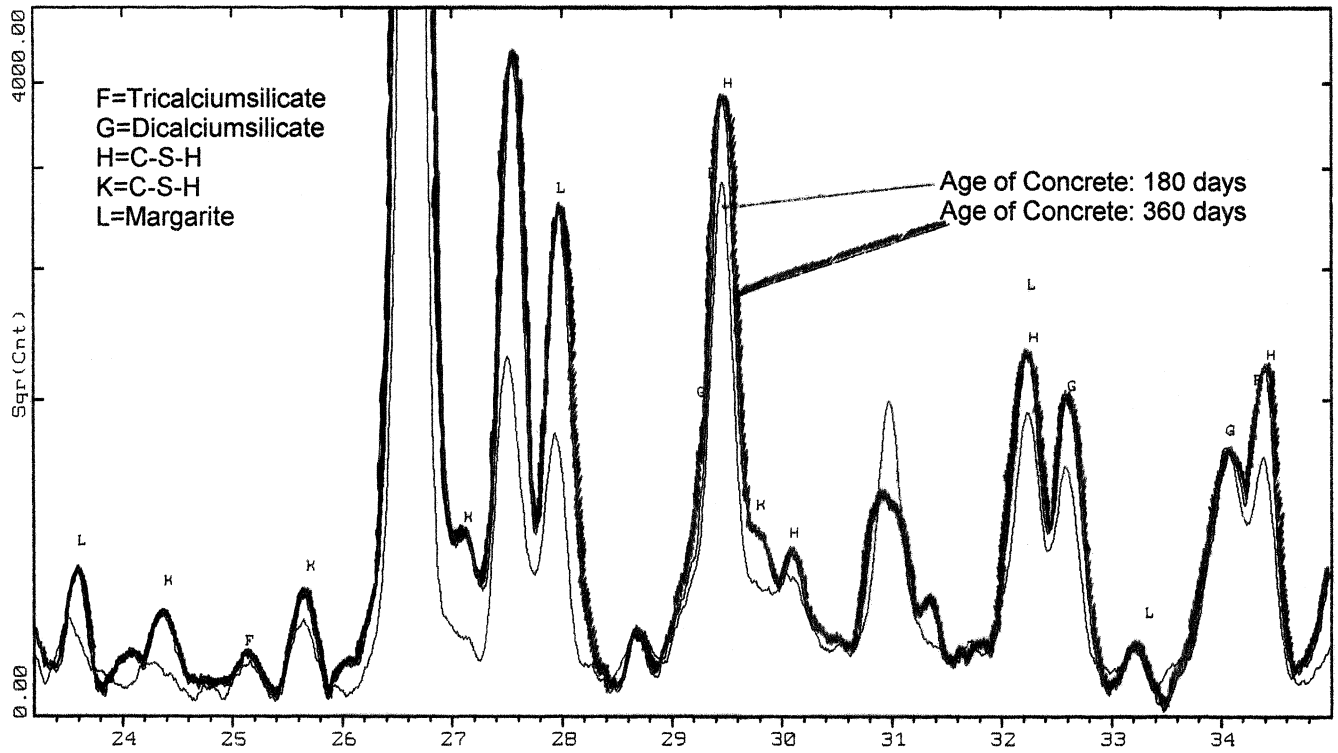

FIGURE 9. X-ray diffraction reflecting angles from 23° to 35°, age of concrete 180 and 360 days.

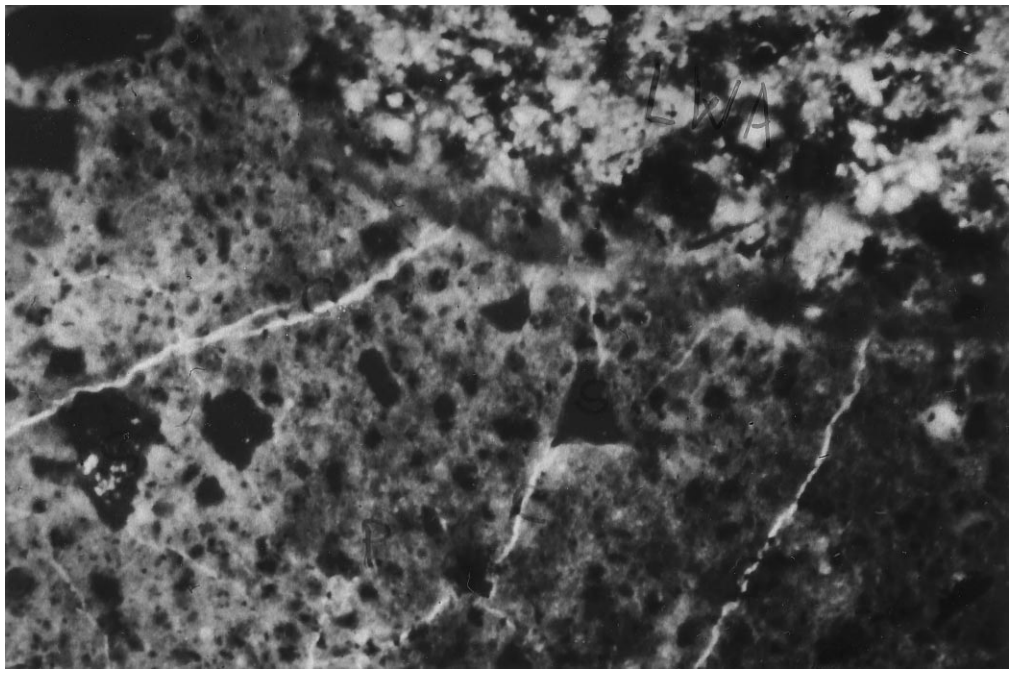

FIGURE 10. Fluorescence microscopy.

of pores with a larger pore radius decreases and the number of pores with smaller radius increases. This confirms the more compact structure of the HCP. It further confirms that the hydration process proceeded, reducing pore sizes and shifting the peak of the distribution curve toward the direction of smaller pores.

Chemical Composition

From the thermal analysis curves it can be seen that, during drying at a relatively low temperature such as 40°, physically bound water as well as chemically bound water is withdrawn. For investigations of the microstructure of high strength concrete, drying at 105°C is inadequate, leading to the discrepancy by calculating the degree of hydration shown in Table 4.

The thermal analyses made on samples stored in a desiccator show a greater amount of chemically bound water at a concrete age of 360 days compared to 180 days. As no water can be supplied from the exterior, the origin of the supplementarily bound water lies in the water content of the LWA.

X-ray diffraction shows more C-S-H of the afwillite type at 360 days compared to 180 days. There is also a greater amount of calcium hydroxide and ettringite observed. The supplementary C-S-H as well as the higher amount of calcium hydroxide and ettringite are the result of supplementary hydration processes.

Conclusion

The concrete presented is a high performance concrete due not only to the recorded high strength but also the insensitivity with respect to inadequate curing. The dryer the curing condition, the higher is the measured compressive strength. Wet curing has no paramount influence on the compressive strength and can, therefore, be neglected.

The microscopic investigation explains the observed improved mechanical properties. The tests performed clearly show a decrease of porosity as a function of time, with the tendency toward smaller pores and, thus, a more compact structure of the cement paste. The more compact structure explains the higher compressive strength.

From the degree of hydration it can be seen that a greater amount of water is chemically bound as the concrete ages. X-ray diffraction analysis shows additional C-S-H, ettringite, and calcium hydroxide. These form only if water is available. Considering the storage condition of the cubes, the LWA is the only possible water supply.

The smaller pores are thus the result of continuous hydration. The additional C-S-H grows into the pores, subdividing them into smaller pores or filling smaller pores. This results in the higher compressive strength observed.

Autogenous Curing

During hydration a system of capillary pores is formed in the cement paste. The radii of these pores

are smaller than the pores of the LWA. As soon as the humidity in the cement paste decreases (due to hydration and drying) a humidity gradient appears. The wet LWA acts as a water reservoir. The pores of the cement paste absorb the water from the LWA by capillary suction. The unhydrated cement particles of the cement paste now have free water to hydrate. The new hydration products grow into the pores of the cement paste, which now become smaller. The capillary suction (being inverse to the square of the radius) increases as the radius becomes smaller and the pores again are able to absorb water from the LWA. This will continue until all the water from the LWA has been transported to the cement paste. Considering this, 1 m^3 of concrete has 47 L of supplementary water for hydration.

Similar to normal concrete exposed to drying, a second humidity gradient appears due to water evaporation, accelerating the appearance of the first humidity gradient. This means that, on the surface of the concrete, the water from the LWA will be used up earlier than in the interior of the concrete. The concrete on the surface becomes more compact in a relatively short time. The lower the relative humidity of the air, the faster this process proceeds. The more compact structure of the concrete surface will reduce the amount of water that normally would evaporate, conserving the water inside the concrete. There are less or no stresses due to drying and, therefore, no microcracks appear.

Acknowledgments

The results are part of a research program that was carried out in the framework of AiF (Co-operative Industrial Research) Project AiF-Nr.9816 and coordinated by DBV (German Concrete Association) Project Nr.178. The support of Liapor Franken, Elkem, and Heidelberger Zement AG is gratefully acknowledged.

References

1. Weber, S.; Reinhardt, H.W. In *Proceedings of the Fourth International Symposium on the Utilisation of High Strength/High Performance Concrete, Vol. 3, Paris, May 29–June 3, 1996*; de Larrard, F.; Lacroix, R., Eds.; 1996; pp 1295–1303.
2. Guse, U. *Dauerhaftigkeit von hochfestem Beton. DAfStb-Forschungskolloquium. Beiträge zum 32. Forschungskolloquium in Karlsruhe am 21. und 22. März 1996*; 1996; pp 99–106.
3. Weber, S. *Ph.D. Thesis*; Stuttgart University: Stuttgart, Germany, 1996.
4. Hasni, L.; Gallias, J.L.; Salomon, M. In *Utilisation of High Strength Concrete, Proceedings, Vol. 2, Symposium in Lillehammer, Norway, June 20–23, 1993*; Holland, I.; Sellevold, E., Eds.; 1993; pp 732–743.
5. Weber, S.; Reinhardt, H.W. In *Durability of High Performance Concrete, RILEM, Cachan 1995*; Sommer, H., Ed.; 1995; pp 59–69.
6. Volkwein, A. *Untersuchungen über das Eindringen von Wasser und Chlorid in Beton. Berichte aus dem Baustoffinstitut TU München*; Heft 1, 1991.
7. *DIN 1164 Zement–Teil 1: Zusammensetzung, Anforderungen*; Ausgabe Oktober 1994.
8. *DIN 1045 Beton und Stahlbeton. Bemessungen und Ausführung*; Ausgabe Juli 1988.
9. *DIN 1048 Prüfverfahren für Beton. Teil 5: Festbeton, gesondert hergestellte Probekörper*; Ausgabe Juni 1991.
10. *EN 196. Methods of Testing Cement. Part 2: Chemical Analysis of Cement*; May 1995.